Using small perturbations to control chaos

Troy Shinbrot, Celso Grebogi, Edward Ott & James A. Yorke

The extreme sensitivity of chaotic systems to tiny perturbations (the 'butterfly effect') can be used both to stabilize regular dynamic behaviours and to direct chaotic trajectories rapidly to a desired state. Incorporating chaos deliberately into practical systems therefore offers the possibility of achieving greater flexibility in their performance.

CHAOTIC systems are characterized by extreme sensitivity to tiny perturbations. This characteristic, known as the 'butterfly effect', is often regarded as a troublesome property, and for many years it has been generally believed that chaotic motions are neither predictable nor controllable. The first reference we find to a differing view is due to John von Neumann, who is reported[1] to have stated around 1950 that small, carefully chosen, pre-planned atmospheric disturbances could lead after some time to desired large-scale changes in the weather. Although this specific application might be problematic, the basic idea of using chaotic sensitivity seems to have been clearly appreciated by von Neumann. Here we review recent work which demonstrates that the butterfly effect permits the use of tiny feedback perturbations to control trajectories in chaotic systems—a capability without a counterpart in nonchaotic systems. These considerations apply to cases in which the chaotic dynamics can in principle be defined by only a few variables, so systems where there are many active degrees of freedom (for example, the weather, and high-Reynolds-number flows) may not be tractable. However, we emphasize that cases of high (or infinite) dimensional systems for which the 'attractor' (and hence the dynamics) is low dimensional are common.

The research that we will review fits broadly into two categories. First we will discuss how, as proposed in ref. 2, one can select a desired behaviour from among the infinite variety of behaviours naturally present in chaotic systems, and then stabilize this behaviour by applying only tiny changes to an accessible system parameter (related work appears in refs 3–32, 77, 78). Moreover, we will show how one can switch between behaviours as circumstances change, again using only tiny perturbations. This means that chaotic systems can achieve great flexibility in their ultimate performance. Second, we will show how one can use the sensitivity of chaotic systems to direct trajectories rapidly to a desired state[33–38]. For example, a few years ago, NASA scientists used only small amounts of residual hydrazine fuel to send the spacecraft ISEE-3/ICE more than 50 million miles across the Solar System, thereby achieving the first scientific cometary encounter[39–43]. This feat was made possible by the sensitivity of the three-body problem of celestial mechanics to small perturbations, and would not have been possible in a nonchaotic system, in which a large effect typically requires a large control[44–46].

Stabilizing unstable orbits

One of the fundamental aspects of chaos is that many different possible motions are simultaneously present in the system. A particular manifestation of this is the fact that there are typically an infinite number of unstable periodic orbits that co-exist with the chaotic motion[47,48]. By a periodic orbit, we mean an orbit that repeats itself after some time (the period). If the system were precisely on an unstable periodic orbit, it would remain on that orbit forever. These orbits are unstable in the sense that the smallest deviation from the periodic orbit (for example due to noise) grows exponentially rapidly in time, and the system orbit quickly moves away from the periodic orbit. Thus, although these periodic orbits are present, they are not typically observed. Rather, what one sees is a chaotic trajectory which bounces around in an erratic, seemingly random fashion. Very rarely, the chaotic trajectory may, by chance, closely approach a particular unstable periodic orbit, in which case the chaotic trajectory would approximately follow the periodic cycle for a few periods, but it would then rapidly move away because of the instability of the periodic orbit. In addition to periodic orbits, it is common for continuous time dynamical systems to have unstable steady states embedded in chaotic motion (see our subsequent discussion of the Lorenz attractor). A ball placed exactly at the top of a hill is an example of an unstable steady state.

Although the existence of steady states and an infinity of different unstable periodic orbits embedded in chaotic motion is not usually obvious in free-running chaotic evolution, these orbits offer a great potential advantage if one wants to control a chaotic system. To demonstrate this, we adopt the following strategy[2]. First we examine the unstable steady states and low-period unstable periodic orbits embedded in the chaotic motion. For each of those unstable orbits, we ask whether the system performance would be improved if that orbit were actually followed. We then select one of the unstable orbits that yields improved performance. Assuming the motion of the free-running chaotic orbit to be ergodic, eventually the chaotic wandering of an orbit trajectory will bring it close to the chosen unstable periodic orbit or steady state. When this occurs, we can apply our small controlling perturbations to direct the orbit to the desired periodic motion or steady state. Moreover, if a small amount of noise is present, we can repeatedly apply the perturba-

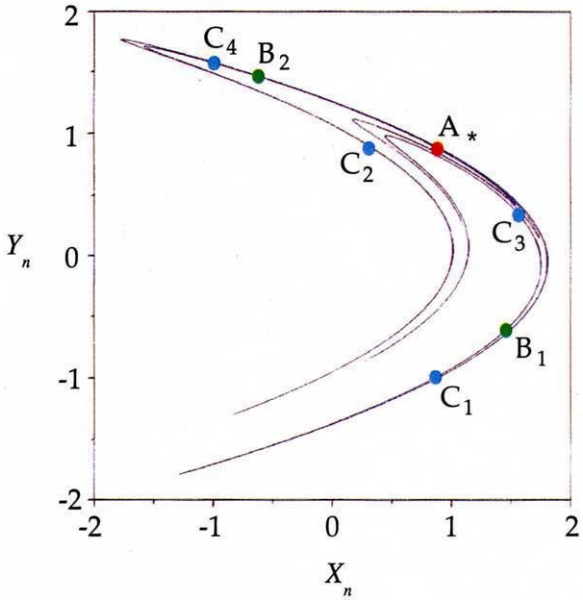

FIG. 1 Hénon attractor, with period-1 point, A_*; period-2 points, B_1 and B_2; and period-4 points, C_1, C_2, C_3 and C_4.

tions to keep the trajectory on the desired orbit. Thus small, carefully chosen perturbations are able to effect a large beneficial change in the long-term system behaviour. If, on the other hand, the system dynamics were not chaotic but were, say, stable periodic, then small controls could only change the orbit slightly. We would then be closely restricted to whatever system performance the stable periodic orbit gave, and we would have no option for improvement using small controls.

Furthermore, one may want a system to be used for different purposes or under different conditions at different times. If the system is chaotic, this requirement might be accommodated without altering the gross configuration of the system. In particular, depending on the use desired, the system could be optimized by switching the temporal programming of the small controls to stabilize different orbits. By contrast, in the absence of chaos, completely separate systems might be required for each use. Thus, when designing a system, it may be advantageous to build chaos in, so as to achieve flexibility. For an experimental example, see Box 1. This experiment couples a magnetic field with a gravitationally buckling ribbon. Other recent relevant experiments have involved laser systems[10–14], electrical circuits[15], thermal convection[16] and arhythmically oscillating cardiac tissue (controlled using a small electrical stimulus)[18].

We will now consider examples of dynamical processes that we wish to control. A simple example might be a metre stick balanced on one's palm. This system is not chaotic and, provided that the stick does not stray too far from the vertical, it can be stabilized in its normally unstable, vertical state by making small motions of one's palm. This is an example of stabilizing an unstable steady state.

As a simple illustrative example of controlling a chaotic system we consider the 'Hénon map'[49]. Here the word 'map' refers to the fact that the time variable is discrete and integer-valued. The Hénon map is also described as a 'two-dimensional map'

BOX 1 Experimental confirmation

THE control of chaos by the application of tiny perturbations has been experimentally applied in several laboratories[14,17,29] (a modification, effective in stabilizing high-period orbits, appears in refs 10, 15). The first such application[9] used a nonlinear, inverted, magneto-elastic ribbon. This ribbon, sketched in Fig. B1, was clamped at its base but was otherwise free to move. The stiffness of the material was nonlinearly dependent on applied magnetic field, and in an oscillating field, applied by external field coils (not shown), the ribbon alternately buckled and stiffened in a complicated, chaotic pattern[76]. The position of the ribbon, $X(t)$, was measured at a point near its base using an optical sensor. By making small adjustments to the amplitude of the oscillating field (variations were less than 9% of its nominal value), the ribbon could be trapped in a variety of periodic motions. Figure B2 shows the ribbon displacement sampled once every oscillation of the applied magnetic field as a function of the number of periods, n. The sampling of the orbit at the drive period can be regarded as a "stroboscopic" surface of section. Initially no control was applied, leading to chaotic variation in the range of ribbon displacements between 2.7 and 4.4 on the vertical axis. Then, at about time $n \cong 2{,}200$, the control algorithm was activated to attempt to stabilize a period-1 orbit in the stroboscopic surface of section (compare this with Fig. 2*b*). After this orbit had been stabilized for over 2,000 oscillations, the control algorithm was switched at time $n \cong 4{,}900$ to try to stabilize a period-2 orbit (see Fig. 2*c*), and was later switched back to the period-1 orbit at $n \cong 7{,}100$.

The nonlinear ribbon was subsequently used to show that chaotic sensitivity can be used to actually direct trajectories in a chaotic system. By making small adjustments to the applied magnetic field (less than 5% of its nominal value), any trajectory could be quickly directed to a small target state. Figure B3 shows several successive trajectories which are rapidly brought from a variety of initial states, indicated by grey circles, to the target neighbourhood, $X = 2.5 \pm 0.01$. This target was chosen because it is ordinarily seldom visited: without control, the time to reach the chosen target was once in 500 iterations on average. By applying small perturbations, on the other hand, the target could typically be reached in less than once every 20 iterations.

We reiterate that the control was accomplished in real time and in the presence of experimental noise and modelling errors (to accommodate this, the targeting algorithm must be periodically reapplied; see refs 33, 35 for details). Additionally, the computational models used both for stabilization and for targeting were constructed entirely from available experimental data and without an *a priori* analytic model.

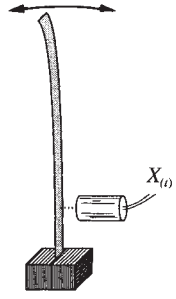

FIG. B1 Chaotic ribbon.

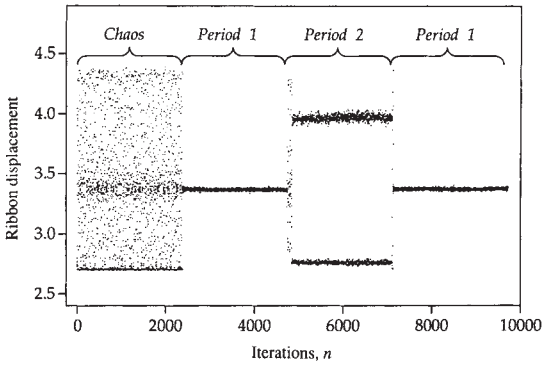

FIG. B2 Experimental stabilization of chaotic ribbon (reprinted with permission from ref. 9).

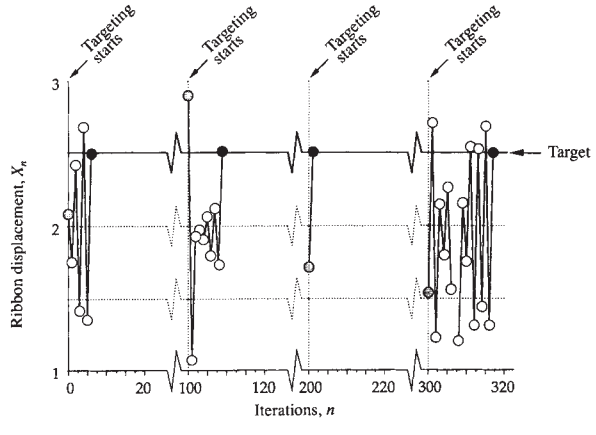

FIG. B3 Several successive realizations of targeting of a small neighbourhood of $X = 2.5$. Ribbon is allowed to wander chaotically between targeting attempts; targeting is initiated at $n = 0, 100, 200, 300$. With targeting, the neighbourhood of $X = 2.5$ is reached within 20 iterations; without targeting, the same neighbourhood is visited less than once every 500 iterations. The origin of the ordinate scale here differs from that of Fig. B2 because the optical sensor was moved between the times of the two experiments.

because the state of the system at time n (where $n = 0, 1, 2, \ldots$) is given by two scalar variables, x_n and y_n. The map specifies a rule for evolving the state of the system at time n to the state at time $(n+1)$. For the Hénon map, this rule is

$$x_{n+1} = p + 0.3y_n - x_n^2 \quad (1a)$$

$$y_{n+1} = x_n \quad (1b)$$

where the parameter p is set to a nominal value of $p_0 = 1.4$. Thus, given an initial state (x_1, y_1), the map allows us to calculate (x_2, y_2), which, when again inserted into the map, yields (x_3, y_3), and so on. Iterations of this map eventually converge to a strange attractor, as shown in Fig. 1. This structure is called an attractor because distant points are drawn toward it under successive iterations of the map, and it is called strange because it is infinitely intricate on every distance scale we might choose to examine. In the terminology of Mandelbrot, it is a fractal and has a fractal dimension of ~1.3. In the figure, we show just a few of the infinite number of embedded unstable periodic orbits; a period-1 point, A_*, which is revisited every map iteration, period-2 points, B_1 and B_2, each of which are revisited every other map iteration ($B_1 \to B_2 \to B_1 \to B_2 \ldots$), and period-4 points, $C_1 \ldots C_4$, which are cycled through every four map iterations.

Although the above example is a map (the time, n, is discrete), many problems in science and engineering involve continuous time, such as a system of M first-order, autonomous ordinary differential equations, $d\boldsymbol{\xi}/dt = \mathbf{G}(\boldsymbol{\xi})$, where $\boldsymbol{\xi}(t) = (\xi^{(1)}(t), \xi^{(2)}(t), \xi^{(3)}(t), \ldots, \xi^{(M)}(t))$ is an M-vector, and the continuous variable t denotes time. In such a case, discrete time systems are still of interest, as the M-dimensional continuous time system can be reduced to an $M-1$ dimensional map by the Poincaré surface-of-section technique illustrated in Fig. 2*a* for $M = 3$. Here we associate the continuous time trajectory with a discrete time trajectory, $\mathbf{Z}_1, \mathbf{Z}_2, \ldots$, where $\mathbf{Z}_n$ denotes an $M-1$ coordinate vector specifying the position on the surface of section of the nth upward piercing of the surface. Given a $\mathbf{Z}_n$, we can integrate the equation $d\boldsymbol{\xi}/dt = \mathbf{G}(\boldsymbol{\xi})$ forward in time from that point, until the next upward piercing of the surface of section, at the surface coordinates $\mathbf{Z}_{n+1}$. Thus $\mathbf{Z}_{n+1}$ is uniquely determined by $\mathbf{Z}_n$, and there must exist a map, $\mathbf{Z}_{n+1} = \mathbf{F}(\mathbf{Z}_n)$, from one trajectory point on the surface of section to the next. Although we may not be able to write down $\mathbf{F}$ explicitly, the knowledge that it exists is still useful. Figure 2*b* shows a periodic orbit of the continuous time system which results in a period-1 orbit of the associated Poincaré surface of section map: $\mathbf{Z}_* = \mathbf{F}(\mathbf{Z}_*)$. Figure 2*c* shows a periodic orbit of the continuous time system resulting in a period-2 orbit of the map: $\mathbf{Z}_2 = \mathbf{F}(\mathbf{Z}_1)$, $\mathbf{Z}_1 = \mathbf{F}(\mathbf{Z}_2)$.

Let us say that we have selected one of these unstable periodic orbits as providing the best performance of some hypothetical system. For simplicity, we consider the case where the desired orbit is a period-1 orbit of some N-dimensional map

$$\mathbf{Z}_{n+1} = \mathbf{F}(\mathbf{Z}_n, p) \quad (2)$$

where $\mathbf{Z}$ is an N-dimensional vector, and p denotes a system parameter. We first approximate the dynamics near the period-1 point, denoted $\mathbf{Z}_*$ (where $\mathbf{Z}_* = \mathbf{F}(\mathbf{Z}_*, p_0)$), for values of the parameter, p, close to the nominal value, p_0, by the linear map

$$(\mathbf{Z}_{n+1} - \mathbf{Z}_*) = \mathbf{A} \cdot (\mathbf{Z}_n - \mathbf{Z}_*) + \mathbf{B} \quad (p - p_0) \quad (3)$$

Here $\mathbf{A}$ is an $N \times N$ dimensional jacobian matrix and $\mathbf{B}$ is an N-dimensional column vector, where $\mathbf{A} = \partial\mathbf{F}/\partial\mathbf{Z}$, $\mathbf{B} = \partial\mathbf{F}/\partial p$, and these partial derivatives are evaluated at $\mathbf{Z} = \mathbf{Z}_*$ and $p = p_0$. We now assume that we can adjust the parameter p on each iteration. That is, we determine $\mathbf{Z}_n$ and on that basis make an appropriate small change in p from the nominal value p_0. Thus we replace p by p_n. Taking the control law to be linear, we have

$$(p_n - p_0) = -\mathbf{K}^T \cdot (\mathbf{Z}_n - \mathbf{Z}_*) \quad (4)$$

Here $\mathbf{K}$ is a constant N-dimensional column vector and $\mathbf{K}^T$ is its transpose. Choice of the vector $\mathbf{K}$ specifies the control law specifying p_n on each iteration. Substituting equation (4) into equation (3), we obtain

$$\delta\mathbf{Z}_{n+1} = (\mathbf{A} - \mathbf{B} \cdot \mathbf{K}^T)\delta\mathbf{Z}_n \quad (5)$$

where $\delta\mathbf{Z}_n = \mathbf{Z}_n - \mathbf{Z}_*$. Thus the period-1 point, $\mathbf{Z}_*$, will be stable if one can choose $\mathbf{K}$ so that the matrix $(\mathbf{A} - \mathbf{B} \cdot \mathbf{K}^T)$ only has eigenvalues with modulus smaller than unity. In this case, $\delta\mathbf{Z}_n \to 0$ (that is, $\mathbf{Z}_n \to \mathbf{Z}_*$) as $n \to \infty$. The choice of $\mathbf{K}$ represents a standard problem in control theory (for example, see ref. 50). (In fact, the matrix $(\mathbf{A} - \mathbf{B} \cdot \mathbf{K}^T)$ can be made to have any desired set of N eigenvalues provided that $\mathbf{B}$ satisfies a certain condition (called controllability[50]).) This procedure gives the time-dependent parameter values, p_n, required to stabilize an unstable period-1 point in a chaotic system. For the case of higher-period orbits, see ref. 4. We imagine that, because of practical constraints, we cannot make the deviations of p_n from p_0 too large. Thus we imagine that $|p_n - p_0|$ is bounded by some allowed maximum value, $\delta p_{\max}$. Hence by equation (4), $\delta p_{\max} > |\mathbf{K}^T \cdot (\mathbf{Z}_n - \mathbf{Z}_*)|$. If the system state is outside this region, we apply no perturbation and wait until the state falls within the

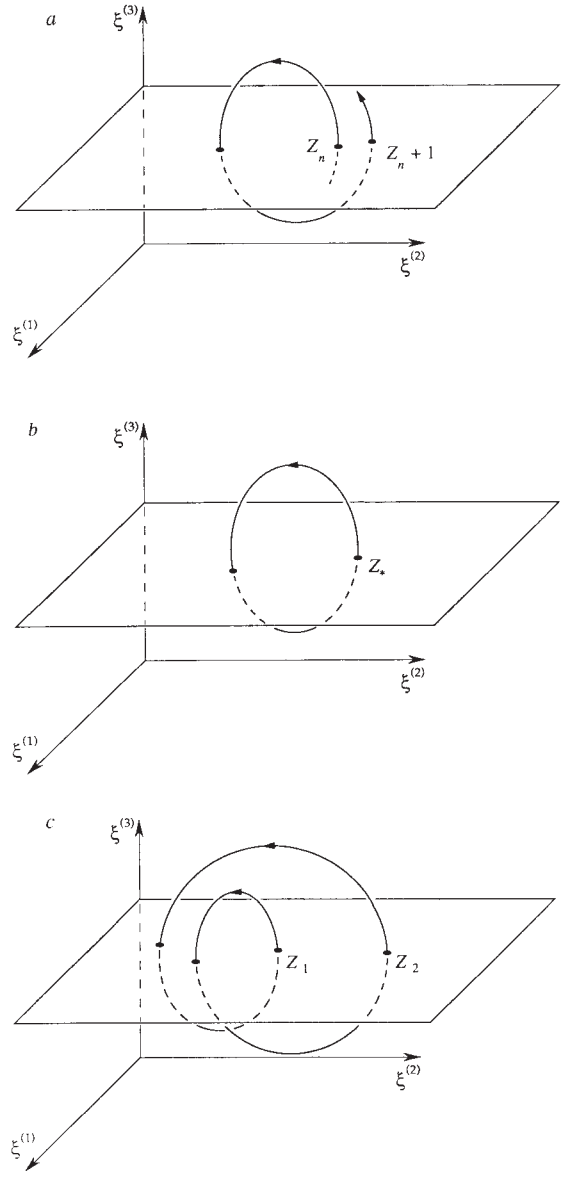

FIG. 2 *a*, The Poincaré surface-of-section technique. The surface of section, here shown for the case ξ_3 = constant, can, in principle, be chosen in any convenient way. *b*, Period-1 orbit; *c*, period-2 orbit.

given region. Once this occurs, we trap the system near the desired periodic state by applying the appropriate small nudges given by equation (4). Stabilization of the periodic points of the Hénon map by small perturbations is similar to stabilizing a vertical metre stick insofar as neither can be accomplished if the current state is far from the desired unstable state. We will discuss later how to direct a chaotic orbit to a neighbourhood of a desired state.

To illustrate stabilization of an unstable period-1 orbit in a more intuitive and geometrical manner, we consider the special case of a two-dimensional map where the desired period-1 orbit has one unstable and one stable direction. That is, there are two curves through $\mathbf{Z}_*$, called the stable manifold and the unstable manifold, as shown in Fig. 3*a*. We consider a small neighbourhood of $\mathbf{Z}_*$, so that the lines shown in Fig. 3 are roughly straight. An orbit starting from a point on the stable manifold remains on the stable manifold and moves exponentially toward $\mathbf{Z}_*$, whereas orbits of points on the unstable manifold move exponentially away from $\mathbf{Z}_*$. This corresponds to the case in which the matrix **A** has two real eigenvalues, one with magnitude less than one (stable), and one with magnitude greater than one (unstable). Also shown in Fig. 3*a* is a dashed line along which $\mathbf{Z}_*$ can be shifted by a change of the parameter p (this line is parallel to the vector **B**).

Imagine that the point $\mathbf{Z}_n$ falls close to $\mathbf{Z}_*(p_0)$, as shown in Fig. 3*a*. We now perturb the value of p from p_0 to $p_0+\delta p$, as shown in Fig. 3*b*. On the next iteration, the orbit is attracted towards $\mathbf{Z}_*(p_0+\delta p)$, in a direction parallel to its stable manifold, and, at the same time, is repelled from $\mathbf{Z}_*(p_0+\delta p)$ in a direction parallel to its unstable manifold. Thus if δp is chosen properly, we can cause $\mathbf{Z}_{n+1}$ to fall precisely on the stable manifold of $\mathbf{Z}_*(p_0)$. Thereafter, we can return the parameter to its nominal value, p_0, and the orbit will remain on the stable manifold of $\mathbf{Z}_*(p_0)$ and will approach $\mathbf{Z}_*(p_0)$. In terms of the more general discussion leading to equations (5), the above corresponds to a special choice of the control vector, **K**, such that one of the eigenvalues of $(\mathbf{A}-\mathbf{B}\cdot\mathbf{K}^T)$ is zero and the other is the original stable eigenvalue of **A**. As shown in ref. 4, this choice is optimal in that it minimizes the average time during which the orbit wanders chaotically before it can be stabilized.

As an example, in Fig. 4, we show the results of stabilizing the periodic orbit, $\mathbf{A}_*$, on the Hénon attractor by adjusting p by less than 1% of its nominal value. Starting at a random initial point on the attractor, we see that for the first 86 iterations, the trajectory moves chaotically on the attractor, never falling within the desired small region about $\mathbf{A}_*$. Then, on the 87th iteration, the state falls within the desired region, and thereafter is held near $\mathbf{A}_*$. In the presence of noise, the stabilization procedure would have to be regularly reapplied (see ref. 3 for details).

The control strategy need not rely on an *a priori* analytical model. Just as one can balance a metre stick on the palm without knowing anything at all about Newton's equations of motion for the stick, one can produce effective stabilization for more complicated systems without an explicit set of differential equations. By empirical study of the effects of small parameter changes on orbits near a desired periodic state, an arbitrary periodic state in a chaotic attractor can be stabilized using only small controls (see Box 1). This is important because in experimental situations one may often not have on hand an accurate analytical model.

Figure 5 illustrates how knowledge of a periodic orbit, the matrix **A**, and the vector **B** can all be extracted purely from observations of the trajectory on the strange attractor. Imagine that we collect a long data string of observed surface-of-section piercings, $\mathbf{Z}_1, \mathbf{Z}_2$ and so on. If two successive **Z**s are close to each other, say $\mathbf{Z}_{100}$ and $\mathbf{Z}_{101}$, then there will typically be a period-1 orbit $\mathbf{Z}_*$ nearby[47,48] (Fig. 5). Having observed a first such close return, we then search the succeeding data for other close-return pairs $(\mathbf{Z}_n, \mathbf{Z}_{n+1})$ restricted to the small region of the original close return (shown shaded in Fig. 5). Because orbits on a strange attractor are ergodic, we will have many such pairs if the data string is long enough. Assuming the shaded region to be small, we then try to fit these close returning pairs with a linear relation

$$\mathbf{Z}_{n+1} = \hat{\mathbf{A}}\cdot\mathbf{Z}_n + \hat{\mathbf{C}} \qquad (6)$$

Generally, if there is noise in the data, we would want to use as many pairs as possible and fit the matrix $\hat{\mathbf{A}}$ and the vector $\hat{\mathbf{C}}$ using a least-squares fit to the data. Thus $\hat{\mathbf{A}}$, the least-squares fit matrix, is an approximation to the jacobian matrix **A** of equation (3), and the period-1 point, $\mathbf{Z}_*(p)$, is approximated by $(1-\hat{\mathbf{A}})^{-1}\cdot\hat{\mathbf{C}}$. To find **B** of equation (3), we change p slightly, $p\to p+\Delta p$, redetermine the period-1 point $\mathbf{Z}_*(p+\Delta p)$ as before, and approximate **B** as $[\mathbf{Z}_*(p+\Delta p)-\mathbf{Z}_*(p)]/\Delta p$. To find period-2 orbits, we proceed in the same way, but for pairs $(\mathbf{Z}_n, \mathbf{Z}_{n+2})$ that are close after two surface-of-section piercings (and similarly for higher periods).

In experimental studies of chaotic dynamics, it is often helpful to use 'delay coordinate embedding'[51,52]. These allow one to obtain information on the topological phase space structure of an attractor even when one cannot directly measure the instantaneous system state vector, ξ, which we take to be M-dimensional. As a typical example, the time history of only a single scalar variable, say $\phi(t)$, might be the only thing that one

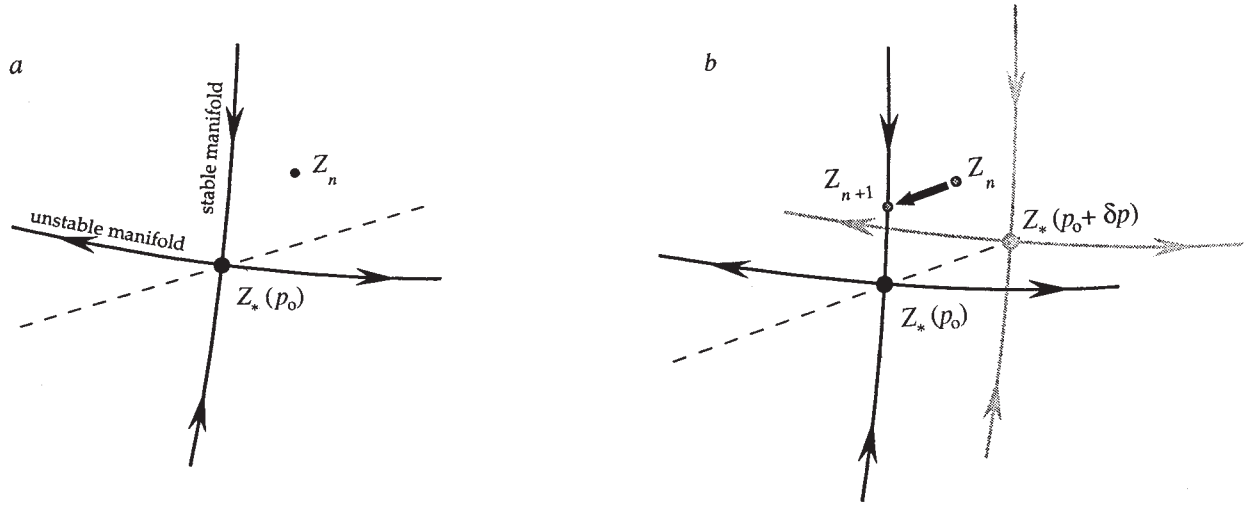

FIG. 3 *a*, The period-1 point, $\mathbf{Z}_*(p_0)$, its stable and unstable manifolds (solid lines), and the line (dashed) along which $\mathbf{Z}_*$ can be shifted by perturbation of the parameter p. *b*, Result of perturbing p to $p_0+\delta p$; the stable and unstable manifolds of $\mathbf{Z}_*(p_0+\delta p)$ are shown as grey lines through $\mathbf{Z}_*(p_0+\delta p)$.

can measure experimentally. To proceed, one forms the Q-dimensional 'delay coordinate vector'

$$\mathbf{\Phi}(t) = (\phi(t), \phi(t - T_D), \phi(t - 2T_D), \ldots, \phi(t - (Q-1)T_D)) \quad (7)$$

where T_D is some conveniently chosen delay time. Embedding theorems[53,54] guarantee that for $Q \geq 2M + 1$, the vector $\mathbf{\Phi}(t)$ is generically a global one-to-one representation of the system state. (Actually, for our purposes we do not require a global embedding; we only require a one-to-one correspondence in the small region near the periodic orbit, and this can typically be achieved with $Q = M$.) To obtain a discrete time series from $\mathbf{\Phi}(t)$, we can again use a Poincaré surface of section, but this time in $\mathbf{\Phi}$-space. Let $\tilde{\mathbf{Z}}_n$ denote points in the $\mathbf{\Phi}$-space surface of section, and let the corresponding surface-of-section map for a constant value of the parameter p be denoted $\tilde{\mathbf{Z}}_{n+1} = \tilde{F}(\tilde{\mathbf{Z}}_n, p)$. As pointed out in ref. 7, in the presence of parameter variation $(p \to p_n)$, delay coordinates lead to a map of a form other than $\tilde{\mathbf{Z}}_{n+1} = \tilde{F}(\tilde{\mathbf{Z}}_n, p_n)$, which is the form assumed for equations (3) and (4). As an example, say that the time interval T_n between the surface-of-section piercing at $\tilde{\mathbf{Z}}_n$ and at $\tilde{\mathbf{Z}}_{n+1}$ is such that

$$rT_n \geq (\mathbf{Q}+1)T_D > (r-1)T_n \quad (8)$$

where r is an integer. Then the relevant map is of the form

$$\tilde{\mathbf{Z}}_{n+1} = \tilde{F}(\tilde{\mathbf{Z}}_n, p_n, p_{n-1}, \ldots, p_{n-r}). \quad (9)$$

This follows because $\mathbf{\Phi}(t_n)$, where t_n denotes the nth piercing of the surface of section (corresponding to $\tilde{\mathbf{Z}}_n$), has components $\phi(t_n), \ldots, \phi(t_n - (Q-1)T_D)$ and hence $\tilde{\mathbf{Z}}_n$ must depend, not only on p_n, but also on all the other parameter values in effect during the time interval $t_n \leq t \leq [t_n - (Q-1)T_D]$. For discussion of how the analysis of equations (3) to (5) can be extended to the case of delay coordinates, see refs 4 and 7.

Although the approach just described provides a systematic means of choosing a feedback algorithm, it will often be the case (particularly when the dynamics are low-dimensional) that a trial and error procedure will succeed[10,15]: simply choose some feedback law (arbitrarily choose **K** in equation (4)) and vary it until it is observed that the desired orbit stabilizes. (Knowledge of the periodic orbit location in phase space is still required, so a procedure such as that of Fig. 5 may still be necessary.)

Further discussion of stabilization

We now briefly discuss some other considerations relevant to the stabilization of unstable periodic orbits and steady states embedded in strange attractors. One issue is related to bifurcations. The word bifurcation, when applied to a periodic orbit or steady state, refers to a change in the character of the orbit from stable to unstable while the system is continuously changed. Often the nset of chaos comes about as a result of bifurcations of periodic orbits or steady states. Two well known cases are the commonly observed cascade of period-doubling bifurcations preceding chaos, and the onset of chaos when a steady state bifurcates from stable to unstable. Thus one way of controlling chaos is to prevent or change the character of these bifurcations. This has been discussed in refs 18 and 19, where control methods that are insensitive to errors in the knowledge of the system are used. In this regard, we also mention the laser experiments of refs 12 and 13.

Control can also be used as a means of tracking the location of unstable orbits as the system is changed[21,22]. In a recent experiment, this technique was used to increase the stable steady power output of a laser by an order of magnitude[17]. Another issue is that of prescribing controls that are assured of bringing the trajectory to the desired periodic orbit or steady state. This has been addressed using the Lyapunov function method[16,23].

Other interesting work in this general area includes the use of the describing function technique of control theory for finding and controlling unstable periodic orbits[24]; control of unstable chaotic sets (as opposed to chaotic attractors)[25]; the control of homoclinic orbits[26]; and control of aperiodic orbits[55].

Directing chaotic trajectories

Stabilizing a system by small perturbations is extremely effective once the system at hand comes close to the desired state. But if it starts far from the desired state, it might take an unacceptably long time before a typical orbit comes close enough to the desired state to be captured. We now discuss how small perturbations, applied when the orbit is far from the desired state, can be used to steer the system to this state. For example, chaotic rhythms in cardiac tissue can be stabilized as outlined above[17]. What if one wants to stabilize a regular rhythm in the heart without having the luxury of simply waiting for the system to fall near a desired state? It is, moreover, intrinsically desirable to be able to steer a system to a general target in phase space (not necessarily a periodic orbit). NASA's mission specialists demonstrated this when, as mentioned earlier, they achieved the first scientific cometary encounter by steering the spacecraft ISEE-3/ICE in a complex trajectory using only small nudges from the spacecraft's dwindling fuel supply[39-43].

The application of chaotic sensitivity to steer trajectories to targets in chaotic systems using small controls is discussed in refs 33-37; related work appears in refs 38 and 55. To understand the idea in its simplest form, consider the well known logistic map (see for example ref. 56):

$$X_{n+1} = pX_n(1 - X_n) \quad (10)$$

where we take a nominal value of 3.9 for p. This map is used to describe the behaviour of a population of organisms after successive years, where n denotes the year. In this case, X represents the (normalized) population, and p defines its growth rate per year when the population is small. For any X between 0 and 1, it is easy, using only a pocket calculator, to adjust the growth rate slightly so that any given target, again between 0 and 1, is quickly reached.

Suppose for example that the current state is $X_1 = 0.4$ and we want to reach the vicinity of $X_n = 0.8$. If we can adjust p during the first year by a small amount, say between 3.8 and 4.0, then after one year, the population can range between $X_2 = 0.91$ and $X_2 = 0.96$. We then return to the nominal parameter value, $p = 3.9$, and after a second year the range grows to cover from $X_3 = 0.15$ to $X_3 = 0.31$. After a third year, the range grows even more to extend from $X_4 = 0.50$ to $X_4 = 0.84$. As our target, $X = 0.8$, is in this range, there must be some value of p_1 in the

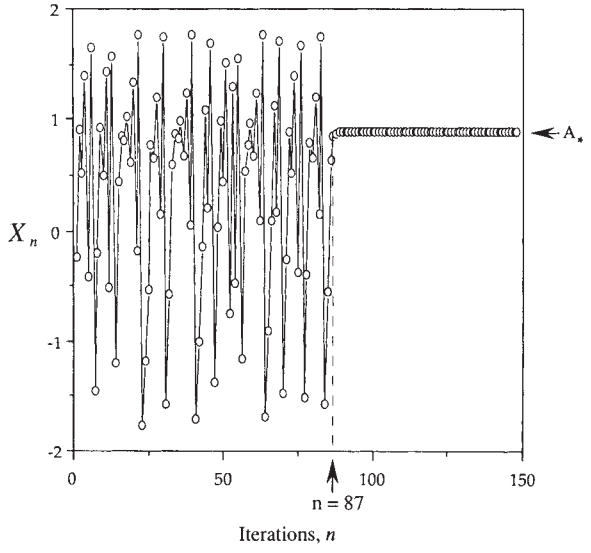

FIG. 4 Stabilization of the period-1 state for the Hénon map.

range $3.8 \leq p_1 \leq 4.0$ such that when p is shifted to that value in the first year, X falls on the target in only three years. Indeed, a little work with our pocket calculator reveals that we can reach our target by setting $p_1 = 3.83189...$. We emphasize that it is possible to accomplish this only because the logistic system is chaotic, and because chaotic systems are characterized by the exponential growth of small disturbances. This exponential growth implies that we can reach any accessible target extremely quickly (that is, in a time of the order of the logarithm of the maximum allowed size of the small parameter perturbation), using only a small perturbation.

As another example, consider the equations

$$\frac{dX}{dt} = \sigma(Y - X) \tag{11a}$$

$$\frac{dY}{dt} = -XY - Y + r + p(t) \tag{11b}$$

$$\frac{dZ}{dt} = XY - bZ \tag{11c}$$

which (for $p(t) \equiv 0$) were introduced[57] by Lorenz as a simplified model of chaotic fluid thermal convection. The Lorenz equations provide a leading-order description of the dynamics of a fluid contained in a thin vertically oriented torus with a heat source applied at the bottom[58]. The equations with $p(t) \equiv 0$ have a strange attractor for the parameter values $\sigma = 10$, $r = 28$, $b = 8/3$, and an orbit on this chaotic attractor is shown in blue in Fig. 6. The steady state, $X(t) = Y(t) = Z(t) = 0$, representing no fluid convection, is a solution of the Lorenz equations. Furthermore, this solution is contained in the chaotic attractor. Note from Fig. 6 that the blue finite-duration orbit does not reach anywhere near this steady state (the open circle in the figure). If the orbit were followed long enough, it would eventually come arbitrarily near the stationary state. We estimate that of the order of one in 10^{10} orbits around either of the lobes of the attractor ever passes through a sphere of radius 0.1 centred at $X = Y = Z = 0$. (For comparison, the blue trajectory in Fig. 6 shows only about 20 orbits around either lobe of the attractor.) For the purpose of demonstrating control of the Lorenz system we have added the term $p(t)$ to the right-hand side of equation (11b). For the physical situation of a vertically oriented fluid-filled torus, the term $p(t)$ represents a perturbation of the position of the heat source slightly to the left or right in the plane of the torus ($p = 0$ corresponds to heating exactly at the bottom of the torus). Restricting the perturbations, $p(t)$, to be small, $|p(t)| < 0.01$, it typically takes of the order of 10 orbits around a lobe to reach the origin (as compared, again, with 10^{10} orbits to reach $\sqrt{X^2 + Y^2 + Z^2} < 0.1$ when no control is applied). Figure 6 shows such an orbit in red. The method for programming the perturbations is described in ref. 36 and is similar in principle to that which we have described for the logistic map, equation (10).

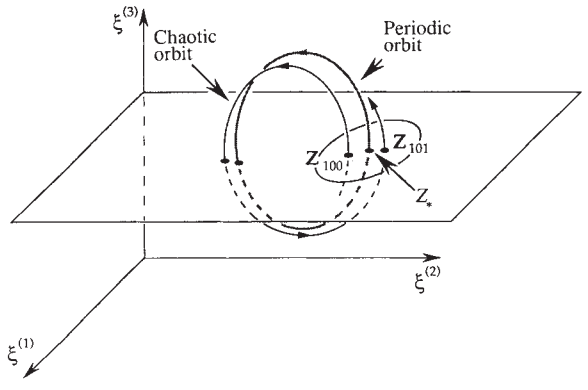

FIG. 5 Determining unstable periodic point, $\mathbf{Z}$ from data, $\mathbf{Z}_{100}$, $\mathbf{Z}_{101}$ ....

The preceding example illustrates the idea of targeting. More detailed descriptions and methods can be found in refs 33–38. One technique is to patch together different trajectories to reach a desired target state. These trajectories can originate in a single chaotic system with differing parameter values[37,38], or from a systematic examination of small changes in the system state[39–43]. NASA's manoeuvre of the spacecraft ISEE-3/ICE is such a case. Five separate swings past the Moon were combined to produce the final spacecraft trajectory. By inventive choices of intermediate trajectories, researchers have shown this technique to be effective in matching greatly differing initial and final state vectors.

At this point, we must make two remarks. First, the sensitivity of chaotic systems allows us to produce large changes in the orbit of the system after some time using tiny perturbations, but the same sensitivity makes the final state depend on ubiquitous noise. The noise, if small enough, can be compensated for, however, by periodically reapplying the targeting algorithm, thereby obtaining mid-course corrections of the parameter perturbation (see Box 1 and refs 33 and 35). Second, one needs a global model of the system in order to direct trajectories. This differs from the stabilization of periodic orbits or steady states, where one only needs local information, near the desired periodic orbit. In general, this makes the use of experimental delay coordinate techniques for application to targeting more difficult. Nevertheless, in some cases it may be possible (Box 1).

The control of chaos by small perturbations has been developed into a proposed application for communication[59]. Consider the 'double scroll' electrical oscillator[60], which yields a chaotic signal consisting of a seemingly random sequence of positive and negative peaks. If we associate a positive peak with a one and a negative peak with a zero, the signal yields a binary sequence. With small control perturbations, we can cause the signal to follow an orbit whose binary sequence represents the information we wish to communicate. (Here our 'target' is a particular binary sequence rather than a point in phase space.) Hence the chaotic power stage that generates the waveform for transmission can remain simple and efficient (complex chaotic behaviour occurs in simple systems), while all the complex electronics controlling the output can remain at the low-power microelectronic level.

Other ways to alter chaotic dynamics

We have focused here on work using the sensitivity of chaotic systems to stabilize existing chosen periodic orbits and steady states and to steer trajectories with only small controls. Several authors have developed other techniques to alter the dynamics of chaotic systems without explicitly using this sensitivity, and in this section, we summarize some of their key contributions.

One body of research[61–68] seeks to control a nonlinear system to follow a prescribed goal dynamics. If we denote the system by

$$\frac{d\boldsymbol{\xi}}{dt} = \mathbf{F}(\boldsymbol{\xi}) + \mathbf{U}(t) \tag{12}$$

where $\mathbf{U}(t)$ is an additive controlling term, then the object is to choose $\mathbf{U}(t)$ so that $|\boldsymbol{\xi}(t) - \mathbf{g}(t)| \to 0$ as $t \to \infty$, where $\mathbf{g}(t)$ is the goal dynamics. To accomplish this, the simple choice

$$\mathbf{U}(t) = \frac{d\mathbf{g}}{dt} - \mathbf{F}(\mathbf{g}(t)) \tag{13}$$

is made. Thus $\boldsymbol{\xi}(t) = \mathbf{g}(t)$ is clearly a solution of the controlled equations. What is not so clear is that convergence to this goal will often occur ($|\boldsymbol{\xi}(t) - \mathbf{g}(t)| \to 0$ as $t \to \infty$). Whether it does so depends on the particular $\mathbf{F}$ and the initial condition, $\boldsymbol{\xi}(0)$. The regions of $\boldsymbol{\xi}$-space such that controlled orbits originating in them converge to the goal, $\mathbf{g}$, are called entrainment regions[64–66]. This method potentially works for nonlinear systems in general (not necessarily chaotic) and has the advantage of not requiring

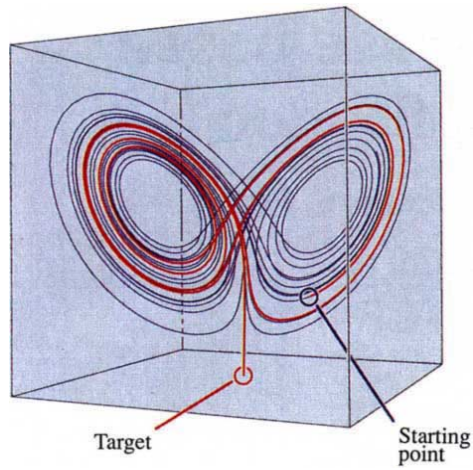

FIG. 6 Targeting of steady state in Lorenz attractor. Blue; trajectory without control; red: trajectory with control.

feedback. On the other hand, the applied controls are not typically small and convergence to the goal is not assured.

Another body of research addresses the effects of periodic[69–73] and stochastic[74,75] perturbations on chaotic systems. As one might expect, the effects of such perturbations can be quite difficult to predict in general, and indeed these studies are not 'goal oriented', in that a desired behaviour is not specified in advance and a generic technique for achieving such a goal has not been developed. Nevertheless, dramatic changes in the dynamics of chaotic systems have been recorded using these methods; for example, periodic or nearly periodic behaviour can sometimes be produced from originally chaotic dynamical systems.

The advantages of chaos

The presence of chaos may be a great advantage for control in a variety of situations. In a nonchaotic system, small controls typically can only change the system dynamics slightly. Short of applying large controls or greatly modifying the system, we are stuck with whatever system performance already exists. In a chaotic system, on the other hand, we are free to choose between a rich variety of dynamical behaviours. Thus we anticipate that it may be advantageous to design chaos into systems, allowing such variety without requiring large controls or the design of separate systems for each desired behaviour.

The general problem of controlling chaotic systems is very rich, and may help solve technologically important problems in widely diverse fields of study. In communications, it has been proposed that chaotic fluctuations can be put to use to send controlled, pre-planned signals[59]. In physiology, applications have been proposed for controlling chaos in the heart[17] and in neural information processing[27]. In fluid mechanics, it has been demonstrated in a simple configuration that chaotic convection[16] can be controlled. Chemical researchers have developed mechanisms for controlling chaotic autocatalytic reactions[28]. Chaotic lasers[10,11] have been controlled, as has the chaotic diode circuit[15]. The wealth of results such as these encourage us to look forward to a fruitful future for the control of chaotic systems. □

Troy Shinbrot is at the Department of Physics and Institute for Physical Science and Technology, University of Maryland, College Park, Maryland 20742, USA; present address for Troy Shinbrot is Laboratory for Fluid Mechanics, Chaos and Mixing, Northwestern University, Evanston, Illinois 60208, USA. Celso Grebogi and James A. Yorke are at the Department of Mathematics and Institute for Physical Science and Technology, University of Maryland, College Park, Maryland 20742, USA. Edward Ott is at the Department of Electrical Engineering, the Department of Physics and the Institute for Systems Research, University of Maryland, College Park, Maryland 20742, USA.

1. Dyson, F. *Infinite in All Directions*, 183–184 (Harper and Row, New York, 1988).
2. Ott, E., Grebogi, C. & Yorke J. A. *Phys. Rev. Lett.* **64,** 1196–1199 (1990).
3. Ott, E., Grebogi, C. & Yorke, J. A. in *Chaos: Soviet–American Perspectives on Nonlinear Science* (ed. Campbell, D. K.) 153–172 (Am. Inst. Phys., New York, 1990).
4. Ott, E., Romeiras, F. J., Grebogi, C. & Dayawansa, W. P. *Physica* D **58,** 165–192 (1992).
5. Auerbach, D., Grebogi, C., Ott, E. & Yorke, J. A. *Phys. Rev. Lett.* **69,** 3479–3482 (1992).
6. Fowler, T. B. *IEEE Trans. Auto. Control* **34,** 201–205 (1989).
7. Dressler, U. & Nitsche, G. *Phys. Rev. Lett.* **68,** 1–4 (1992).
8. Pyragas, K. *Phys. Lett.* A**170,** 421–428 (1992).
9. Ditto, W. L., Rauseo, S. N. & Spano, M. L. *Phys. Rev. Lett.* **65,** 3211–3214 (1990).
10. Roy, R., Murphy, T. W., Maier, T. D., Gills, A. & Hunt, E. R. *Phys. Rev. Lett.* **68,** 1259–1262 (1992).
11. Gills, Z., Iwata, C., Roy, R., Schwartz, I. B. & Triandaf, I. *Phys. Rev. Lett.* **69,** 3169–3172 (1992).
12. Bielawski, S., Bouazaoui, M., Derozier, D. & Glorieux, P. *Proc. Nonlinear Dynam. Optical Syst. Topical Mtg, Alpbach, Austria, June 22–26* (Optical Society of America, Washington, DC 1992).
13. Bielawski, S., Bouazaoui, M., Derozier, D. & Glorieux, P. *Stabilization and Characterization of Unstable Steady States in a Laser* (preprint, 1992).
14. Reyl, C., Flepp, L., Badii, R. & Brun, E. *Control of NMR-laser Chaos in High-dimensional Embedding Space* (preprint, 1992).
15. Hunt, E. R. *Phys. Rev. Lett.* **67,** 1953–1955 (1991).
16. Singer, J., Wang, Y. Z. & Bau, H. H. *Phys. Rev. Lett.* **66,** 1123–1125 (1991).
17. Garfinkel, A., Spano, M. L., Ditto, W. L. & Weiss, J. N. *Science* **257,** 1230–1235 (1992).
18. Abed, E. H., Wang, H. O. & Lee, H.-C. *Proc. 1992 Am. Control Conf.*, 2236–2237 (Chicago, 1992).
19. Wang, H. O. & Abed, E. H. *Proc. 2nd IFAC Workshop Syst. Struct. Control*, 494–497 (Prague, 1992).
20. Wang, H. O. & Abed, E. H. *Proc. 2nd IFAC Nonlinear Control Sys. Design Symp.*, 57–62 (Bordeaux, France, June 1992).
21. Schwartz, I. B. & Triandaf, I. *Phys. Rev.* A**46,** 7439–7444 (1992).
22. Carroll, T., Triandaf, I., Schwartz, I. B. & Pecora, L. *Phys. Rev.* A**46,** 6189–6192 (1992).
23. Chen, G. & Dong, X. *J. Circ. Syst. Comput.* **3** (in the press).
24. Genesio, R. & Tesi, A. *Automatica* **28,** 531–548 (1992).
25. Tél, T. *J. Phys.* A**24,** L1359–L1368 (1992).
26. Bloch, A. M. & Marsden, J. E. *Theor. comput. Fluid Dynam.* **1,** 179–190 (1989).
27. Ding, M. & Kelso, J. A. S. in *Measuring Chaos in the Human Brain* (eds Duke, D. & Pritchard, W.) 17–31 (World Scientific, Singapore, 1991).
28. Petrov, V., Gáspár, V., Masere, J. & Showalter, K. *Nature* **361,** 240–243 (1993).
29. Hübinger, B., Doerner, R. & Martienssen, W. *Controlling Chaotic Motion in Noisy Systems* (preprint, Phys. Inst. der J. W. Goethe-Universität, Frankfurt-am-Main, 1992).
30. Vassiliadis, D. *Physica* D (in the press).
31. Huberman, B. A. & Lumer, E. *IEEE Trans. Circ. Syst.* **37,** 547–550 (1990).
32. Sinha, S. & Ramaswamy, R. *Physica* D**43,** 118–128 (1990).
33. Shinbrot, T., Ott, E., Grebogi, C. & Yorke, J. A. *Phys. Rev. Lett.* **65,** 3215–3218 (1990).
34. Shinbrot, T., Ott, E., Grebogi, C. & Torke, J. A. *Phys. Rev.* A**45,** 4165–4168 (1992).
35. Shinbrot, T., Ott, E., Grebogi, C. & Yorke, J. A. *Phys. Rev. Lett.* **68,** 2863–2866 (1992).
36. Shinbrot, T., Grebogi, C., Ott, E. & Yorke, J. A. *Phys. Lett.* A**169,** 349–354 (1992).
37. Kostelich, E., Grebogi, C., Ott, E. & Yorke, J. A. *Phys. Rev.* E**47,** 305–310 (1993).
38. Bradley, E. in *Lecture Notes Control and Information Sciences*, No. 165 (eds Jacob, G. & Lamnabhi-Lagarrigue, F.) 307–325 (Springer, Berlin, 1991).
39. Farquhar, R., Muhonen, D. & Church, L. C. *J. astronaut. Sci.* **33,** 235–254 (1985).
40. Muhonen, D., Davis, S. & Dunham, D. *J. astronaut. Sci.* **33,** 255–273 (1985).
41. Dunham, D. W. & Davis, S. A. *J. astronaut. Sci.* **33,** 275–288 (1985).
42. Muhonen, D. & Folta, D. *J. astronaut. Sci.* **33,** 289–300 (1985).
43. Efron, L., Yeomans, D. K. & Schanzle, A. F. *J. astronaut. Sci.* **33,** 301–323 (1985).
44. So, P., Ott, E. & Dayawansa, W. P. *Phys. Lett.* A. (in the press).
45. Chen, G. & Dong, X. *From Chaos to Order—Perspectives and Methodologies in Controlling Chaotic Dynamical Systems Tech. Rep. 92-07* (Univ. Houston, Texas, 1992).
46. Vincent, T. L. & Yu, J. *Dynam. Control* **1,** 35–52 (1991).
47. Grebogi, C., Ott, E. & Yorke, J. A. *Phys. Rev.* A**37,** 1711 (1988).
48. Auerbach, D., Cvitanović, P., Eckmann, J.-P., Gunaratne, G. & Procaccia, I. *Phys. Rev. Lett.* **58,** 2387 (1987).
49. Hénon, M. *Commun. Math. Phys.* **50,** 69–77 (1976).
50. Ogata, K. *Modern Control Engineering*, 2nd Ed. 347–889 (Prentice-Hall, Englewood Cliffs, 1990).
51. Packard, N. H., Crutchfield, J. P., Farmer, J. D. & Shaw, R. S. *Phys. Rev. Lett.* **45,** 712–716 (1980).
52. Eckmann, J.-P. & Ruelle, D. *Rev. mod. Phys.* **57,** 617–656 (1985).
53. Whitney, H. *Ann. Math.* **37,** 645–671 (1936).
54. Takens, F. in *Lecture Notes in Mathematics 898* (eds Rand, D. A. & Young, L. S.) 366–381 (Springer, Berlin, 1981).
55. Mehta, N. J. & Henderson, R. M. *Phys. Rev.* A**44,** 4861–4865 (1991).
56. Schuster, H. G. *Deterministic Chaos*, 2nd ed., 37–38 (VCH, Weinheim, 1989).
57. Lorenz, E. *J. atmos. Sci.* **20,** 130–141 (1963).
58. Yorke, J. A., Yorke, E. D. & Mallet-Paret, J. *Physica* D**24,** 279–291 (1987).
59. Hayes, S., Grebogi, C. & Ott, E. *Phys. Rev. Lett.* **70,** 3031–3034 (1993).
60. Chua, L. O., Komura, M. & Matsumoto, T. *IEEE Trans. Circ. Syst.* **11,** 1073–1118 (1986).
61. Hübler, A. & Lüscher, E. *Naturwissenschaften* **76,** 67–69 (1989).
62. Hübler, A. W. *Helv. phys. Acta* **62,** 343–346 (1989).
63. Plapp, B. B. & Hübler, A. W. *Phys. Rev. Lett.* **65,** 2302–2305 (1990).
64. Jackson, E. A. & Hübler, A. W. *Physica* D**44,** 407–420 (1990).
65. Jackson, E. A. *Phys. Lett.* A**151,** 478–484 (1990).
66. Jackson, E. A. *Phys. Rev.* A**44,** 4839–4853 (1991).
67. Lüscher, E. & Hübler, A. W. *Helv. phys. Acta* **62,** 544–551 (1989).
68. Georgii, R., Eberl, W. & Lüscher, E. *Helv. phys. Acta* **62,** 290–293 (1989).
69. Alekseev, V. V. & Loskutov, A. Y. *Sov. Phys. Dokl.* **32,** 1346–1348 (1987).
70. Pettini, M. in *Dynamics and Stochastic Processes* (ed. Lima, R., Streit, L. & Vilela Mendes, R. 242–250 (Springer, Berlin, 1990).
71. Lima, R. & Pettini, M. *Phys. Rev.* A**41,** 726–733 (1990).
72. Braiman, Y. & Goldhirsch, I. *Phys. Rev. Lett.* **66,** 2545–2548 (1991).
73. Azevedo, A. & Rezende, S. M. *Phys. Rev. Lett.* **66,** 1342–1345 (1991).
74. Herzel, H. *A. Angew. Math. Mech.* **68,** 11–12 (1988).
75. Fahy, S. & Hamann, D. R. *Phys. Rev. Lett.* **69,** 761–764 (1992).
76. Ditto, W. L. *et al. Phys. Rev. Lett.* **63,** 923–966 (1989).
77. Lai, Y.-C., Ding, M.-Z. & Grebogi, C. *Phys. Rev.* E**47,** 86–92 (1992).
78. Abed, E. H., Wang, H. O. & Chen, R. *Physica* D (in the press).

ACKNOWLEDGEMENTS. This work was supported by the United States Department of Energy (Office of Scientific Computing, Office of Energy Research). We thank D. Auerbach, G. R. Chen, A. Hübler and K. Scarbrough for helpful comments. W. Ditto, S. Rauseo and M. Spano are gratefully acknowledged for providing data for this article.